Octahedral complexes of the series of actinides hexafluorides AnF$_6$

Andrea Pérez-Villa [a], Jorge David [b], Patricio Fuentealba [c,d], Albeiro Restrepo [a,*]

[a] Grupo de Química-Física Teórica, Instituto de Química, Universidad de Antioquia, AA 1226 Medellín, Colombia
[b] Escuela de Ciencias y Humanidades, Departamento de Ciencias Básicas, Universidad Eafit, AA 3600 Medellín, Colombia
[c] Departamento de Física, Facultad de Ciencias, Universidad de Chile, Casilla 653, Santiago 1, Chile
[d] Centro para el Desarrollo de la Nanociencia y la Nanotecnología, CEDENNA, Avenida Ecuador 3493, Santiago, Chile

ARTICLE INFO

ABSTRACT

Non-relativistic DFT (PW91, PBE, PB86) geometry optimizations followed by relativistic ZORA single point energy calculations on the neutral hexafluoride complexes of the series of actinides U, Np, Pu, Am, Cm, Bk, Cf, Es, Fm, Md, No, Lr in octahedral symmetry are presented. Bond lengths are in good agreement with available experimental data. Actinide bond length contraction as a function of the atomic number of the central metal atom of up to $\approx 4\%$ is observed. An approximate inverse relationship is predicted for the bonding energies as a function of the atomic number of the central cation at the two component ZORA//DFT level; pure DFT bonding energies do not exhibit the same pattern.

© 2011 Elsevier B.V. All rights reserved.

1. Introduction

The chemistry of the compounds of the series of actinides is interesting for both practical and fundamental reasons. Actinides chemistry has practical implications in nuclear technology and in the handling and disposal of nuclear waste [1]. Actinides are interesting from a fundamental point of view because of contributions from 5f orbitals to bonding [1]. Sophisticated calculations on actinides compounds are now possible because of the advances in technology that produce faster and better computers. However, despite the advances in experimental and computational techniques, many structural and chemical properties of the compounds of the actinide series remain unexplored [2].

According to Molski and Seppelt [3], a total of 16 binary element hexafluorides are known, out of which three are actinide hexafluoride compounds: UF$_6$, NpF$_6$, PuF$_6$. Among the binary hexafluorides, SF$_6$ and UF$_6$ are extremely well studied. A triplet, octahedral $(5dt_{2g})^4$ geometry for PtF$_6$ was predicted by Wesendrup and Schwerdtfeger [4] using scalar relativistic DFT and Coupled Clusters methods. UF$_6$, an important part of the nuclear fuel cycle is one of the most frequently studied actinide systems. Single crystal structures of a series of metal hexafluorides (Mo, Tc, Ru, Rh, W, Re, Os, Ir, and Pt) at −140 °C were reported by Drews and coworkers [5]. All compounds were shown to crystallize under the same molecular structure exhibiting octahedral symmetry. Gagliardi and coworkers [6] studied via a variety of theoretical methods the structures of UF$_6$ and PuF$_6$ monomers and dimers, finding little differences between the geometries of the monomers. The three

known actinide hexafluorides have been studied under a wide variety of theoretical methods: see for example calculations on UF$_6$ [7–17], calculations on NpF$_6$ [13] and calculations on PuF$_6$ [13,18]. There are additional reports on molecular dynamics simulations on the solvation of UCl$_6^{3-}$, UCl$_6^{2-}$, UCl$_6^{-}$ [19].

Experimental data on the structures of UF$_6$, NpF$_6$, PuF$_6$ can be found in several works [20–23]. Garrison and Becnel [24] studied the UF$_6$ + H$_2$O reaction because it is important to understand the corrosion caused by the HF produced, which can significantly degrade the tanks commonly used for storage and because UF$_6$ is highly toxic, and the thermochemistry of its hydrolysis reaction plays an important role in its environmental dispersion. Hydrolysis and solvation of the AnCl$_6^{2-}$ complexes (An = U, Np, Pu) have also been studied [25–27]. Synthesis of AmF$_6$ has been elusive. Fitzpatrick and coworkers [28], for example, following the same steps for the preparation of PuF$_6$, attempted fluorination of AmF$_4$ with O$_2$F without success. Other methodologies including reactions of solid Am with F$_2$, ClF$_3$ and BF$_3$ [29] and with KrF$_2$ [30] proved to be ineffective as well for the production of AmF$_6$.

In this Letter, we study the geometries, molecular properties, and relativistic effects for the octahedral complexes of the series of actinides hexafluorides AnF$_6$, An = U (Z = 92) to Lr (Z = 103). Accurate computations in compounds of the actinide series are notoriously difficult due to several, wide in scope reasons; we cite the following among the most relevant:

(i) *Relativistic effects*: Pyykkö has pointed out that for the existing actinoids, relativistic effects are essential [31]. It has been shown that the high electronegativity of fluorine atoms magnifies the relativistic effects when bonded to heavy metals [32]. M-X bond lengths decrease from La-X, Ac-X to Lu-X,

* Corresponding author.
  E-mail address: albeiro@matematicas.udea.edu.co (A. Restrepo).

Lr-X, respectively. It is worth noticing that the actinide contraction of the monoxide (AcO) is entirely a relativistic effect; i.e., at the non-relativistic level a slight actinide expansion is obtained [2,33]. It is known that bonds formed by f elements sometimes show a relativistic bond length expansion, as opposed to the more commonly observed contraction in non-f elements [31,34,35]. Several cases have been reported in which relativistic effects influence molecular geometries, we cite a few: PdF_6, PtF_6 and DsF_6 [36], CH_2ICl^+ [37], WF_5 [38], UF_5 [39], Co_6^-, Rh_6^-, Ir_6^- [40]. On the other hand, Schreckenbach and Shamov suggest that for UF_6 and $U_2O_2F_2$, GGA functionals provide accurate geometries and frequencies while hybrid functionals are superior for energetics [1].

(ii) *Jahn–Teller distortions*: Jahn–Teller (JT) molecular geometry distortions of hexa-coordinated transition metal compounds are well established, especially when there is degeneracy on the orbitals of partially filled d valence shells; the statement translates into the series of actinides for the cases of degeneracy of partially filled f shells. Complex combinations of JT effects and spin–orbit (SO) couplings are needed for correct description of molecular geometries [41,42]. A very recent report [40] suggests that JT distortions are a case of incomplete theory for d^4 complexes: as Z for the central cation increases, the SO couplings approach the magnitudes of D_q, the Crystal Field splitting parameters for the square bipyramid, D_{4h} geometries, resulting from distortions of O_h octahedral geometries. Molecular geometry distortions due to the dynamic JT effect are usually treated within a non-relativistic theoretical framework. One popular approach to account for JT distortions and SO couplings is to avoid solving the full relativistic Dirac Hamiltonian by diagonalizing the vibronic Hamiltonian (linear, quadratic JT) and then include the SO couplings via perturbations. Such line of action, when applied to study molecules with C_{3v} geometries, led Berckholtz and Miller to conclude 'The necessity of performing the complete calculation becomes clear as the deviations between approximation and reality becomes large' [43]. A more sophisticated approach, involving the vibronic Hamiltonian describing linear JT and SO couplings in the diabatic spin–orbital representation, employing the Breit–Pauli SO couplings in the single electron approximation, has been used for example in the treatment of trigonal symmetry molecules [44]. To our knowledge, there are only two reports of attempts to include the SO coupling effects by solving the full relativistic Dirac Hamiltonian in four-component space [36,40]; in both cases, the relativistic calculations lead to the experimental O_h symmetries, while at the non-relativistic limit, distorted D_{4h} geometries are predicted, that is, JT distortions for PdF_6, PtF_6, DsF_6, CoF_6^-, RhF_6^- and IrF_6^- are a consequence of neglecting the SO couplings.

(iii) *Inner shell correlation effects*: for heavier elements, electron correlation is especially strong because as electrons come closer to each other, there is a growing number of orbitals sharing the same region of space [2].

(iv) *The number of allowed microstates for partially filled f shells*: The number of microstates for n electrons to be spread among m spin–orbitals is given by the binomial coefficient. Because of symmetry and several types of couplings, not all the possible microstates have physical meaning, however, the number of possibilities to be computed is quite large. The maximum number of f microstates for the metal cations in the complexes studied here corresponds to the Es^{6+} cation, which with a minimal basis set, would allow 3432 microstates to accommodate 7f electrons in 14 spin–orbitals.

2. Computational details

Following Schreckenbach and Shamov's suggestion [1] (see above), we attempted molecular geometry optimization for octahedral symmetry complexes in the series of actinides hexafluorides AnF_6 (An = U, Np, Pu, Am, Cm, Bk, Cf, Es, Fm, Md, No, Lr) by using the PW91, PBE, PB86 functionals in conjunction with a triple zeta plus polarization (TZP) basis set. The TZP basis set for the series of actinides contains Slater functions up to an angular momentum $\ell = 5$. Calculations were run under the frozen core approximation, (no core pseudopotentials involved); we set the frozen cores to 80 electrons (5d) for the actinides and to 2 electrons (1s) for F atoms. Molecular geometry optimizations were carried out by forcing the AnF_6 systems to reamain in O_h symmetry. Characterization of all the molecular species as true minima or saddle points was carried out by calculating second derivatives at the same optimization level. Relativistic effects at the two component zeroth-order regular approximation, ZORA [45], were considered via single point energy calculations with the same TZP basis set. The ZORA Hamiltonian includes SO interactions and partially recovers the relativistic kinetic energy; since the relativistic kinetic energy is positive, ZORA is known to yield too negative absolute energies [41]; in addition, it is known that ZORA is not electrostatically gauge invariant, leading to erroneous distortions of molecular geometries due to non physical forces between nuclei [46]. To our knowledge, the ZORA implementation in ADF by van Lenthe and coworkers [47], uses the scaled ZORA Hamiltonian, which according to the authors "is exactly gauge invariant for hydrogenic ions. It is practically gauge invariant for many-electron systems and proves superior to the (unscaled) first order regular approximation for atomic ionization energies. The regular approximation, if scaled, can therefore be applied already in zeroth order to molecular bond energies." The authors presented, among several pieces of evidence to support their claim, deviations between scaled ZORA and full four component Dirac Hamiltonian calculations no larger than 0.08% for the energies of valence orbitals levels in Uranium; no larger than 3×10^{-3}% in total energies for Gold and Uranium atoms; and no larger than 0.03% in ionization energies for Gold. Finally, the authors state that the scaled ZORA Hamiltonian is specially adequate for valence orbitals [47], like the ones used in our frozen core calculations. A gauge-invariant formulation of ZORA was recently given by Filatov and Cremer [46]. In this Letter, we use the ADF-2008 suite of programs [48] and its implementation of ZORA and the PW91, PBE and PB86 functionals for all calculations.

3. Results and discussion

3.1. Geometries

Octahedral symmetry molecular geometries for the series of actinides hexafluorides AnF_6 were optimized using the computational methods described above. Not all octahedral molecular species are well defined minima within the calculated potential energy surfaces (PES): AmF_6, MdF_6, NoF_6 converged to octahedral equilibrium geometries for all chosen functionals, however, were predicted to exhibit negative eigenvalues of the Hessian matrix; this results are not discouraging in view of the lack of experimental evidence for the existence of the involved hexafluorides and of the failed attempts to synthesize AmF_6 mentioned above [28–30].

A summary of An-F bond lengths for the octahedral complexes is listed in Table 1. A contraction trend to a maximum of $\approx 4\%$ of the An-F bond length is observed as the atomic number of the metal increases (except for LrF_6); this result is consistent with the well documented actinide contraction [31,34,35]. Our calculations show good agreement with experimental bond lengths for UF_6

Table 1
M–F bond lengths (Å) for the series of actinides hexafluorides. Available experimental values: $R_U - F = 1.999$ Å [21–23]; $R_{Np} - F = 1.980$ Å [23]; $R_{Pu} - F = 1.972$Å[23,6]. The ADF program predicts AmF_6, MdF_6, NoF_6, not to be well defined minima under O_h symmetry for any of the studied functionals (see text).
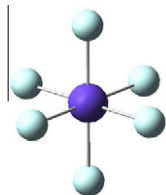
Complex	NR-PW91	NR-PBE	NR-BP86
UF_6	1.97	1.96	1.95
NpF_6	1.93	1.93	1.92
PuF_6	1.94	1.93	1.92
AmF_6	1.90	1.91	1.89
CmF_6	1.91	1.91	1.90
BkF_6	1.91	1.89	1.87
CfF_6	1.90	1.90	1.88
EsF_6	1.95	1.88	1.87
FmF_6	1.91	1.90	1.88
MdF_6	1.97	1.94	1.92
NoF_6	2.04	2.04	2.01
LrF_6	1.97	1.93	1.92

and PuF_6 and are not inferior to prior theoretical studies [6,7], so we feel confident in applying the same methodology to the unreported hexafluorides.

3.2. Energetics and bonding

Bonding energies are computed as the difference between the fragments and the complex as implemented in ADF. Bonding energies calculated in this way lead to larger positive numbers for the more stable complexes. Table 2 shows bonding energies for all AnF_6 complexes. The bonding energies reported here exhibit deviations from experimental binding energy values already pointed out in other non-relativistic calculations: Gagliardi and coworkers for example [6], reported 23.11 eV for all electron non-relativistic atomization energies in UF_6 (experimental value 32.55 eV [21]; our bonding energies are 44.3, 44.4 eV (Table 2)). There is an approximate inverse relationship between the atomic number of the central cation and the ZORA calculated bonding energies as shown in Figure 1; pure DFT calculations do not reproduce the same behavior, instead, a low → high → low··· trend in the bonding energies is predicted for alternating even → odd → even···it Z of the central cation; this probably has to do with symmetry breaking due to Jahn–Teller effect, which is compensated by the SO couplings in the relativistic case [41]. The largest bonding energy

Table 2
Bonding energies (eV) for the series of actinides hexafluorides. Available experimental binding energy values: $BE_{UF_6} = 31.91$ eV[21–23]; $BE_{NpF_6} = 29.35$ eV[23]; $BE_{PuF_6} = 26.85$ eV[23,6]. The ADF program predicts AmF_6, MdF_6, NoF_6, not to be well defined minima under O_h symmetry for any of the studied functionals (see text).

| Complex	NR-PW91	NR-PBE	NR-BP86	ZORA//PW91	ZORA//PBE	ZORA//BP86
UF_6	44.9	44.7	44.3	45.2	44.9	44.4
NpF_6	47.7	47.4	47.1	44.2	44.0	43.5
PuF_6	38.5	38.3	38.0	42.0	41.7	41.1
AmF_6	42.8	42.5	42.1	39.5	39.4	38.9
CmF_6	45.7	45.4	45.1	42.4	42.2	41.8
BkF_6	43.4	43.5	43.4	36.8	36.3	35.7
CfF_6	38.9	38.6	38.6	34.2	34.0	33.3
EsF_6	48.0	51.9	51.7	31.8	32.2	31.8
FmF_6	35.7	35.8	36.1	30.6	30.2	29.6
MdF_6	39.6	42.4	43.5	28.7	28.1	27.7
NoF_6	30.8	30.5	32.5	26.2	25.9	25.6
LrF_6	51.1	55.5	55.6	31.2	30.3	30.0
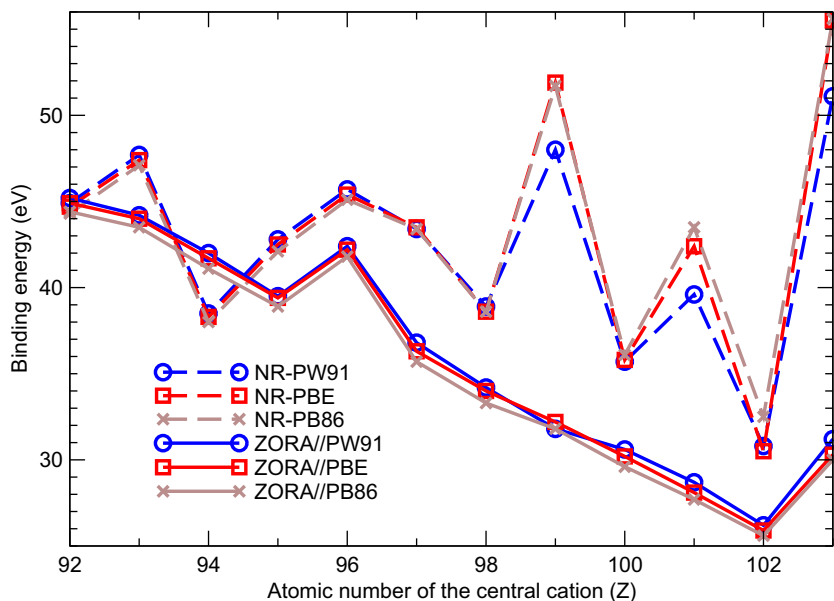
Fig. 1. Bonding energies as a function of the atomic number of the central cation. An approximate inverse Z dependency for the ZORA//DFT bonding energies is observed; no such trend is predicted by NR-DFT calculations.
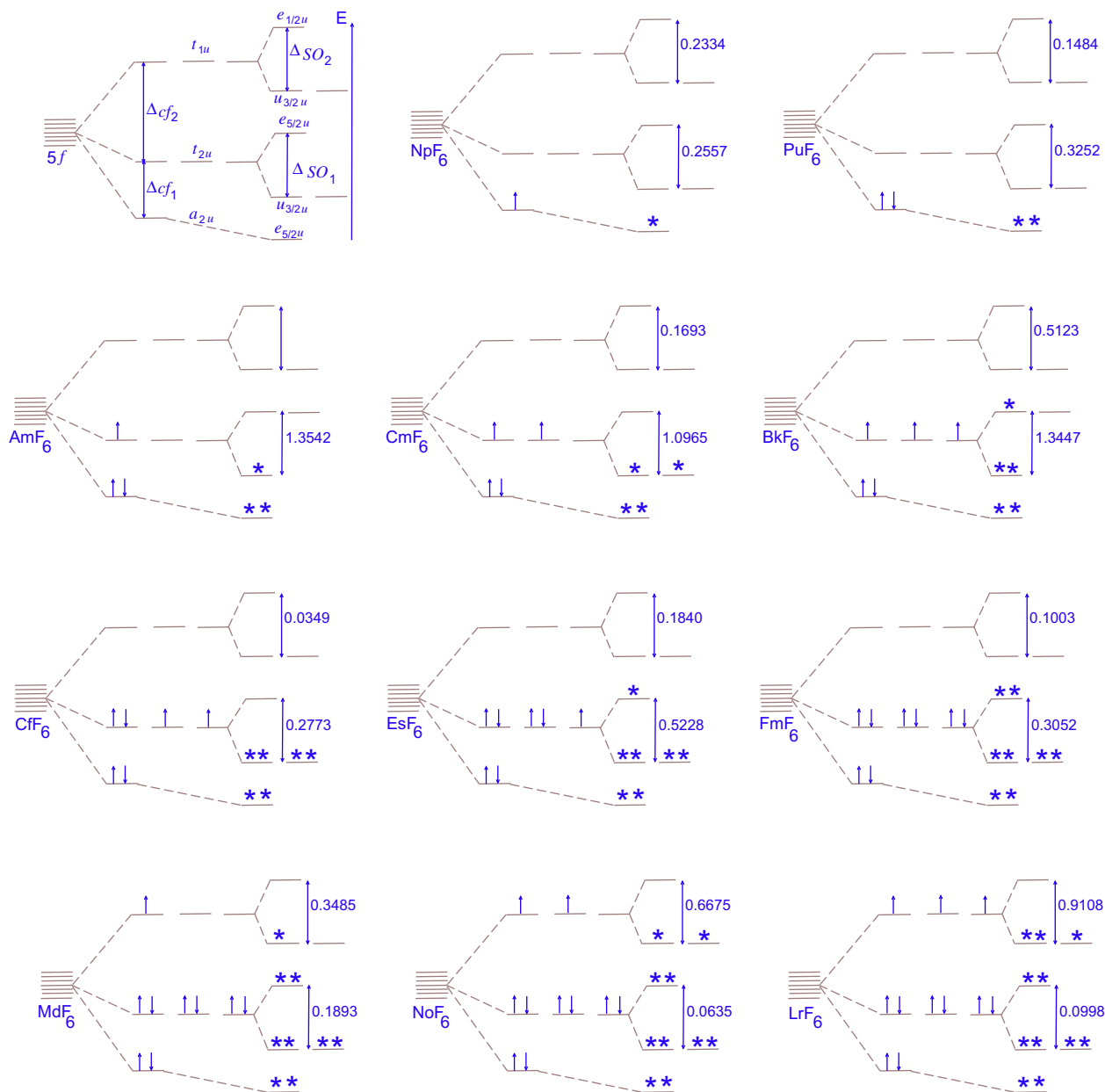
Fig. 2. BP86 and ZORA//BP86 Energy splittings (eV) of the 5f orbitals under octahedral fields and under the influence of the spin–orbit couplings. UF$_6$, a system with no f electrons in the central cation is not shown. BkF$_6$, CfF$_6$, LrF$_6$ reduce their spin multiplicity under relativistic treatment; notice that the u_{3u} orbitals are destabilized with respect to the $e_{\frac{5}{2}u}$ orbitals in AmF$_6$ and BkF$_6$. Energy differences are not drawn to scale to help visualization. For the open shell systems, the unrestricted calculations predict small differences in energies for the α and β spin–orbitals, they are drawn as degenerate for simplicity. The ADF program predicts AmF$_6$, MdF$_6$, NoF$_6$, to be not well defined minima under O$_h$ symmetry for any of the studied functionals (see text).

(more stabilized) hexafluoride is UF$_6$ at the ZORA//DFT levels, while LrF$_6$ is the most stable at pure DFT levels. A remarkable consistency is observed: non-relativistic calculations reproduce the same trend regardless of the functional used, while all ZORA// DFT calculations also follow a different trend. The significant DFT and ZORA overestimation of experimental binding energies and their mutual disagreement reveal that energy calculations on the title AnF$_6$ series are more sensitive to inclusion of electron correlation and/or relativistic formalism than geometrical parameters, for which very good results are obtained in this Letter (see above).

3.3. Splitting of the 5f orbitals

Crystal field theory (CFT) dictates that octahedral fields split the f orbitals into the a_{2u}, t_{2u}, t_{1u} irreducible representations. For the

relativistic case, in the double group symmetry (O_h^*), the extrairreducible representations for the f shell, $e_{\frac{5}{2}u}$, $u_{\frac{3}{2}u}$, $e_{\frac{5}{2}u}$, $u_{\frac{3}{2}u}$, $e_{\frac{1}{2}u}$, are afforded by the direct products

$$\Gamma_{\text{spin}} \otimes a_{2u} = e_{\frac{5}{2}u}, \quad \Gamma_{\text{spin}} \otimes t_{2u} = u_{\frac{3}{2}u} \oplus e_{\frac{5}{2}u}, \quad \Gamma_{\text{spin}} \otimes t_{1u} = u_{\frac{3}{2}u} \oplus e_{\frac{1}{2}u}$$

$$(1)$$

From the CFT splittings, a further division of the 3 dimensional representations into a 2 dimensional and a 1 dimensional representations is expected because of the effect of the SO couplings. A generic diagram for the PB86 and ZORA//PB86 splittings of the 5f orbitals including definitions for the several energy differences is shown in Figure 2. Figure 3 shows the variation of the magnitudes of the SO couplings as a function of Z of the central cation. several interesting observations are drawn from Figures 2 and 3: (i) As a
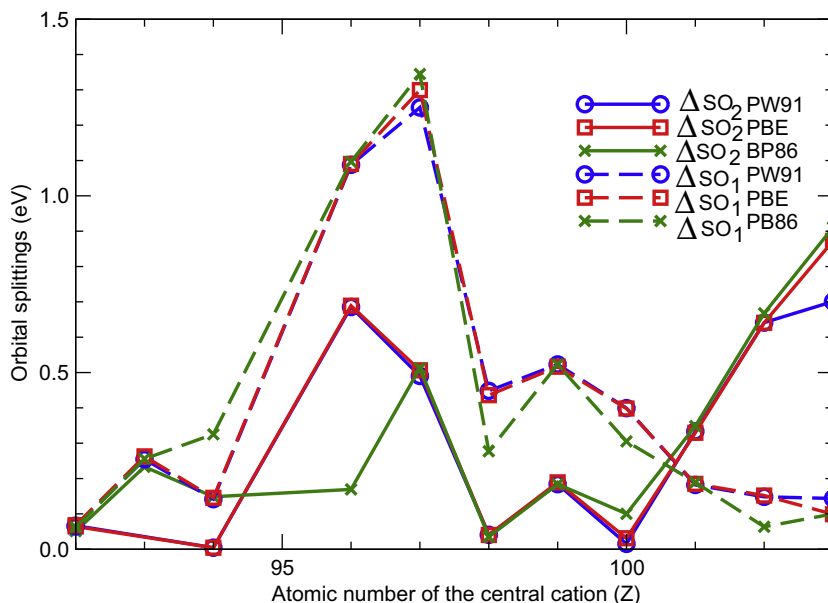
Fig. 3. Calculated splittings (eV) of the $5f$ orbitals under octahedral fields for the AnF$_6$ series.

Table 3

Electron configurations for the series of AnF$_6$. The leftmost superscript indicates the predicted spin multiplicity; superscripts to the right indicate the number of electrons on a given orbital (see Figure 2). All non-relativistic functionals afforded the same electron configurations for a given central cation. For MdF$_6$, NoF$_6$, LrF$_6$, slightly different electron configurations are predicted by the ZORA//PBE and ZORA//PB86 calculations; only the ZORA//PW91 results are listed. The ADF program predicts AmF$_6$, MdF$_6$, NoF$_6$, not to be well defined minima under O$_h$ symmetry for any of the studied functionals (see text).

complex	NR-DFT	ZORA//PW91
UF$_6$	$^1(a_{2u}^0)$	$^1\left(e_{\frac{5}{2}u}^0\right)$
NpF$_6$	$^2(a_{2u}^1)$	$^2\left(e_{\frac{5}{2}u}^1\right)$
PuF$_6$	$^1(a_{2u}^2)$	$^1\left(e_{\frac{5}{2}u}^2\right)$
AmF$_6$	$^2(a_{2u}^2 t_{1u}^1)$	$^2\left(e_{\frac{5}{2}u}^2 e_{\frac{1}{2}u}^1\right)$
CmF$_6$	$^3(a_{2u}^2 t_{2u}^2)$	$^3\left(e_{\frac{5}{2}u}^2 u_{\frac{3}{2}u}^2\right)$
BkF$_6$	$^4(a_{2u}^2 t_{2u}^3)$	$^2\left(e_{\frac{5}{2}u}^2 e_{\frac{5}{2}u}^2 u_{\frac{3}{2}u}^1\right)$
CfF$_6$	$^3(a_{2u}^2 t_{2u}^4)$	$^1\left(e_{\frac{5}{2}u}^2 u_{\frac{3}{2}u}^4\right)$
EsF$_6$	$^2(a_{2u}^2 t_{2u}^5)$	$^2\left(e_{\frac{5}{2}u}^2 u_{\frac{3}{2}u}^4 e_{\frac{1}{2}u}^1\right)$
FmF$_6$	$^1(a_{2u}^2 t_{2u}^6)$	$^1\left(e_{\frac{5}{2}u}^2 u_{\frac{3}{2}u}^4 e_{\frac{1}{2}u}^2\right)$
MdF$_6$	$^2(a_{2u}^2 t_{2u}^6 t_{1u}^1)$	$^2\left(e_{\frac{5}{2}u}^2 u_{\frac{3}{2}u}^4 e_{\frac{1}{2}u}^2 u_{\frac{3}{2}u}^1\right)$
NoF$_6$	$^3(a_{2u}^2 t_{2u}^6 t_{1u}^2)$	$^3\left(e_{\frac{5}{2}u}^2 u_{\frac{3}{2}u}^4 e_{\frac{5}{2}u}^2 u_{\frac{3}{2}u}^2\right)$
LrF$_6$	$^4(a_{2u}^2 t_{2u}^6 t_{1u}^3)$	$^2\left(e_{\frac{5}{2}u}^2 u_{\frac{3}{2}u}^4 e_{\frac{5}{2}u}^2 u_{\frac{3}{2}u}^3\right)$

their total spin multiplicities under the ZORA treatment; this result is a consequence of large stabilizations of the $u_{\frac{3}{2}u}$ spinors, which restrain the electrons from occupying the higher energy $e_{\frac{5}{2}u}$, $e_{\frac{1}{2}u}$ orbitals.

4. Conclusions and perspectives

We present non-relativistic hybrid DFT (PW91, PBE, PB86) geometry optimizations followed by two-component ZORA single point energy calculations on the optimized geometries of the series of actinides hexafluorides AnF$_6$, An = U, Np, Pu, Am, Cm, Bk, Cf, Es, Fm, Md, No, Lr. Not all hexafluorides are well defined minima within the corresponding PES: AmF$_6$, MdF$_6$, NoF$_6$ could not be characterized as minima with any functional (there is no experimental evidence for the existence of any of them). There is $\approx 4\%$ contraction on the series of An–F bond lengths. An approximate inverse relationship is predicted for the bonding energies as a function of the atomic number of the central cation at the ZORA//DFT levels; pure DFT bonding energies do not exhibit the same pattern. Somewhat large SO couplings are predicted in most cases, resulting in a reduction of the relativistic total molecular spin multiplicity for BkF$_6$, CfF$_6$, and LrF$_6$ and providing additional stabilization to all octahedral molecular geometries.

References

[1] G. Schreckenbach, G. Shamov, Acc. Chem. Res. 43 (2010) 19.
[2] M. Dolg, in: P.V.R. Schleyer, N.L. Allinger, T. Clark, J. Gasteiger, P.A. Kollman, H.F. Schaefer III, P.R. Schreiner (Eds.), Encyclopedia of Computational Chemistry, Wiley, Chichester, 1998, p. 1478.
[3] M. Molski, K. Seppelt, Dalton Trans. (2009) 3379.
[4] R. Wesendrup, P. Schwerdtfeger, Inorg. Chem. 40 (2001) 3351.
[5] T. Drews, J. Supel, A. Hagenbach, K. Seppelt, Inorg. Chem. 45 (2006) 3782.
[6] L. Gagliardi, A. Willets, C. Skylaris, N. Handy, A. Spencer, A. Ioannou, A. Simper, J. Am. Chem. Soc. 120 (1998) 11727.

general norm, $\Delta_{SO_1} > \Delta_{SO_2}$, the crossing point occurring beyond FmF$_6$ (ii) curves for Δ_{SO_1} have approximately the same shapes as for Δ_{SO_2}, with different magnitudes (iii) progressive filling of the f orbitals leads to increase in Δ_{SO_2} and decrease in Δ_{SO_1} beyond CfF$_6$, in other words, completely filling the $u_{\frac{3}{2}u}$ extrairreducible representations coming from the t_{2u} orbitals, partially responsible for Δ_{SO_1}, seems to be a transition point between two approximately increasing trends for Δ_{SO_2} and between approximately increasing to approximately decreasing trends in Δ_{SO_1}. (iv) The somewhat large SO couplings predicted in this Letter provide extra stabilization to the octahedral molecular geometries, very much in agreement with what has been found for d^4 complexes [40].

Table 3 summarizes the electron configurations and spin multiplicities for all AnF$_6$ predicted in this Letter. BkF$_6$, CfF$_6$, LrF$_6$ reduce

[7] W. De Jong, W. Nieuwpoort, Int. J. Quantum Chem. 58 (1996) 203.
[8] P. Hay, J. Chem. Phys. 79 (1983) 5469.
[9] S. Larsson, J. Tse, J. Esquivel, A. Tang, Chem. Phys. 89 (1984) 43.
[10] A. Soldatov, Zh. Strukt. Khim. 26 (1985) 3.
[11] J. Onoe, K. Takeuchi, H. Nakamatsu, T. Mukoyama, R. Sekine, H. Adachi, Chem. Phys. Lett. 196 (1992) 636.
[12] J. Onoe, K. Takeuchi, H. Nakamatsu, T. Mukoyama, R. Sekine, H. Adachi, J. El. Spetr. Rel. Phen. 60 (1992) 29.
[13] P. Hay, R. Martin, J. Chem. Phys. 109 (1998) 3875.
[14] G. Malli, J. Styszynski, J. Chem. Phys. 104 (1996) 1012.
[15] J. Onoe, K. Takeuchi, H. Nakamatsu, T. Mukoyama, R. Sekine, B. Kim, H. Adachi, J. Chem. Phys. 99 (1993) 6810.
[16] I. Parsons, S. Till, J. Chem. Soc. Faraday Trans. 89 (1993) 25.
[17] E. Batista, R. Martin, P. Hay, J. Peralta, G. Scuseria, J. Chem. Phys. 121 (2004) 2144.
[18] W. Wadt, J. Chem. Phys. 86 (1987) 339.
[19] R. Schurhammer, G. Wipff, J. Phys. Chem. B 111 (2007) 4659.
[20] F. Kraus, S. Baer, Chem. Eur. J. 15 (2009) 8269.
[21] A. Freeman, C. Keller (Eds.), Handbook of Chemistry and Physics of Actinides, Elsevier, New York, 1986.
[22] H. Seip, Acta Chem. Scand. 19 (1965) 1955.
[23] N. Galkin, Y. Tumanov, Russ. Chem. Rev. 40 (2) (1971) 154.
[24] S. Garrison, J. Becnel, J. Phys. Chem. A 112 (2008) 5453.
[25] E. Bossé, C. Den Auwer, C. Berthon, P. Guilbaud, M. Grigoriev, S. Nikitenko, C. Le Naour, C. Cannes, P. Moisy, Inorg. Chem. 47 (13) (2008) 5746.
[26] S. Nikitenko, C. Cannes, C. Le Naour, P. Moisy, D. Trubert, Inorg. Chem. 44 (2005) 9497.
[27] S. Nikitenko, P. Moisy, Inorg. Chem. 45 (2006) 1235.
[28] J. Fitzpatrick, J. Dunn, L. Avens, United States, Patent Number 4710222, 1987.
[29] J. Gibson, R. Haire, J. Alloys Compounds 181 (1992) 23.
[30] L. Asprey, P. Eller, S. Kinkead, Inorg. Chem. 25 (1986) 670.
[31] P. Pyykkö, Chem. Rev. 88 (1988) 563.
[32] J. David, A. Restrepo, Phys. Rev. A 76 (2007) 052511.
[33] W. Küchle, M. Dolg, H. Stoll, J. Phys. Chem. A 101 (1997) 7128.
[34] P. Pyykkö, Adv. Quantum Chem. 11 (1978) 353.
[35] M. Seth, M. Dolg, P. Fulde, P. Schwerdfeger, J. Am. Chem. Soc. 117 (1995) 6597.
[36] J. David, P. Fuentealba, A. Restrepo, Chem. Phys. Lett. 457 (2008) 42.
[37] M. Lee, H. Kim, Y. Lee, M. Kim, Angew. Chem. Int. Ed. 44 (2005) 2929.
[38] K. Dyall, J. Phys. Chem. A 104 (2000) 4077.
[39] J. Onoe, H. Nakamatsu, T. Mukoyama, R. Sekine, H. Adachi, K. Takeuchi, Inorg. Chem. 36 (1997) 1934.
[40] J. David, D. Guerra, A. Restrepo, Inorg. Chem. 50 (2011) 1480.
[41] K. Dyall, K. Faegri, Introduction to Relativistic Quantum Chemistry, Oxford, New York, 2007, p. 467.
[42] I. Bersuker, Cambridge University Press, Cambridge, U. K., 2010.
[43] T. Berckholtz, T. Miller, Int. Rev. Phys. Chem. 17 (1998) 435.
[44] W. Domcke, S. Mishra, L. Poluyanov, Chem. Phys. 322 (2006) 405.
[45] Ch. Chang, M. Pélissier, P. Durand, Phys. Scri. 34 (1986) 394.
[46] M. Filatov, D. Cremer, J. Chem. Phys. 122 (2005) 044104.
[47] E. van Lenthe, E. Baerends, J. Snijders, J. Chem. Phys. 101 (1994) 9783.
[48] Amsterdam Density Functional (ADF) code. release 2008: Vrije Universiteit: Amsterdam, The Netherlands, 2008.